



Synthesis and characterization of Ce and La modified bismuth titanate

Nikolina Pavlović^{1,*}, Dejan Kancko¹, Katalin Mészáros Szécsényi², Vladimir V. Srdić¹

¹Department of Material Engineering, Faculty of Technology, University of Novi Sad, Bul. Cara Lazara 1, 21000 Novi Sad, Serbia

²Department of Chemistry, Faculty of Sciences, University of Novi Sad, Trg Dositeja Obradovica 2, 21000 Novi Sad, Serbia

Received 1 November 2008; received in revised form 19 April 2009; accepted 21 May 2009

Abstract

Bismuth titanate based nanopowders with the different content of La or Ce were synthesized by the modified sol-gel method. After calcination at 600°C, in addition to Aurivillius layered structure, a small quantity of cubic pyrochlore phase was detected in the La modified powders, while this second phase was much more pronounced in the Ce substituted powders. In fact, as the powder with the highest amount of Ce ($\text{Bi}_3\text{CeTi}_3\text{O}_{12}$) has the pure pyrochlore phase it seems that the presence of Ce stabilizes the formation of this phase. This different influence of cerium and lanthanum could be explained by the incorporation of their ions on the different sites in the titanate structure. Bismuth titanate based ceramics, sintered at 1050°C/2h, had densities above 93% of theoretical density and characteristic plate-like grain morphology. Small quantity of cubic pyrochlore phase was detected only in the Ce modified bismuth titanate ceramics. On the other hand, lanthanum addition caused formation of smaller grain size with pronounced plate-like morphology.

Keywords: bismuth titanate, lanthanum, cerium, powder synthesis, sintering

1. Introduction

Bismuth titanate, $\text{Bi}_{4-x}\text{A}_x\text{Ti}_3\text{O}_{12}$ (BT), as a ferroelectric material with its high Curie temperature (675°C), excellent fatigue endurance and electro-optic switching, has attracted considerable attention for application in non-volatile ferroelectric random access memory, high-temperature piezoelectric and electro-optical devices. The structure of these ferroelectrics can be described as the intergrowth of fluorite-like $[\text{M}_2\text{O}_2]^{2+}$ units and perovskite-like $[\text{A}_{n-1}\text{B}_n\text{O}_{3n+1}]^{2-}$ blocks. In the general formula of the Aurivillius family, n is the number of BO_6 octahedra, (i.e. $n = 1-5$), A represents 12-fold cation sites which can be occupied by Ba^{2+} , Ca^{2+} , Sr^{2+} , Bi^{3+} and the rare earth cations while on 6-fold B sites belonging to BO_6 octahedra Ti^{4+} , Ta^{5+} , Nb^{5+} and W^{6+} can be found. The $[\text{M}_2\text{O}_2]^{2+}$ layers (M being 8-coordinated) were only thought to be occupied by Bi^{3+} , leading to alternate layers of fixed ideal charges, $[\text{Bi}_2\text{O}_2]^{2+}$ and $[\text{A}_{n-1}\text{B}_n\text{O}_{3n+1}]^{2-}$ [1,2] The three-layer member ($n = 3$) of Aurivillius phase is bismuth titanate, $\text{Bi}_4\text{Ti}_3\text{O}_{12}$.

The plate-like morphology, typical for this kind of structure and the presence of hard agglomerates from the conventional method of synthesis result in low sinterability of the powder and poor properties of the final $\text{Bi}_4\text{Ti}_3\text{O}_{12}$ ceramic products. In order to decrease calcination temperature and to improve reactivity of raw materials and homogeneity of the obtained powder, many wet-chemical methods such as sol-gel method, hydrothermal and coprecipitation have been used.

In bismuth titanate it is possible to substitute cations of the proper ionic radii for A, B and/or M sites. Thus, the structure of BT has been modified with different cations, such as W^{6+} , La^{3+} , Nb^{5+} , Ce^{3+} , Ta^{5+} etc., which can change the structure and morphology of BT ceramics and enhance the electric/ferroelectric properties [3–5]. But, besides $\text{Bi}_4\text{Ti}_3\text{O}_{12}$, several other phases in the Bi-Ti-O system can be formed, such as $\text{Bi}_2\text{Ti}_2\text{O}_7$ [6], $\text{Bi}_2\text{Ti}_4\text{O}_{11}$, $\text{Bi}_{12}\text{TiO}_{20}$, $\text{Bi}_8\text{TiO}_{14}$ [7] and so on. $\text{Bi}_2\text{Ti}_2\text{O}_7$ belongs to the compounds of the general formula $\text{A}_2\text{B}_2\text{O}_7$ representing cubic pyrochlore structure. Pyrochlore oxides are predominantly ionic in nature and lend themselves to a wide variety of chemical substitution at the A and B sites, provided ionic radius and chemical neu-

* Corresponding author: tel: +381 21 485 3750
fax: +381 21 450 413, e-mail: nikolinapavlovic@yahoo.com

trality criteria are satisfied [8]. Pyrochlore can also host mixed-valence metals such as $\text{Fe}^{2+}/\text{Fe}^{3+}$, $\text{Nb}^{4+}/\text{Nb}^{5+}$ and $\text{Ce}^{3+}/\text{Ce}^{4+}$ [9].

In the present work the influence of different amounts of La and Ce on the structure, morphology and sintering behavior of bismuth titanate based powders was investigated.

II. Experimental

Ce- and La- substituted bismuth titanate ceramics were prepared from nanopowders having the following compositions $\text{Bi}_{4-x}\text{A}_x\text{Ti}_3\text{O}_{12}$ (where $A = \text{La}$ or Ce and $x \leq 1$, with the sample notations - BT, BCT- y and BLT- y where $y = 100 \cdot x$). Bismuth titanate nanopowders were synthesized by the modified sol-gel method in a two-step process: first by controlled hydrolysis of titanium-butoxide ($\text{Ti}(\text{OC}_4\text{H}_9)_4$, Fluka) with distilled water, and then by further reaction of the formed hydrated titania gel particles with corresponding ions (Bi^{3+} and La^{3+} or Ce^{3+}). The homogeneous solutions containing corresponding quantities of bismuth and cerium or lanthanum ions were obtained by dissolution of nitrate precursors ($\text{Bi}(\text{NO}_3)_3 \cdot 5\text{H}_2\text{O}$, Fluka, $\text{Ce}(\text{NO}_3)_3 \cdot 6\text{H}_2\text{O}$, Merck and $\text{La}(\text{NO}_3)_3 \cdot 6\text{H}_2\text{O}$, Riedel-de Haen) in concentrated nitric acid. The $\text{Bi}^{3+}/\text{Ce}^{3+}$ and $\text{Bi}^{3+}/\text{La}^{3+}$ solutions were mixed in previously prepared amorphous titania sol and the reaction between them was carried out under a highly basic conditions (6M NaOH), at room temperature and continuous stirring for 1 hour. The precipitated particles were washed with distilled water and absolute ethanol and finally dried at 120°C overnight.

The obtained as-synthesized powders were calcined at 600°C for 1 hour and uniaxially pressed in a hard metal die with diameter of 10 mm, at room temperature and compaction pressures of 125 MPa. The pressed pellets were heated with a heating rate of $10^\circ\text{C}/\text{min}$ and sintered at 1050°C for two hours in the Bi_2O_3 rich atmosphere in a closed crucible. The $\text{Bi}_4\text{Ti}_3\text{O}_{12}$ powder placed in the crucible is used as a source of the bismuth oxide in order to minimize the bismuth loss during high-temperature sintering.

Thermal behaviour of the as-synthesized samples was examined by simultaneous differential thermal analysis (DTA) and thermogravimetric analysis (TG) up to 800°C on SDT Q600 and Bähr STA 503 in air atmosphere, at a heating rate of $10^\circ\text{C}/\text{min}$. Al_2O_3 was used as the reference material. Infrared spectra were collected by FTIR spectrometer (NEXUS 670 FT-IR) for the range of wavelengths from 400 to 4000 cm^{-1} . Specific surface areas were determined based on isotherms of low-temperature nitrogen adsorption using the BET method (Micrometrics ASAP 2000). Particle size and morphology of the bismuth titanate based powders after calcinations at 600°C in addition to quality analyses were determined using scanning electron microscopy, SEM (JEOL JSM-6460LV) and EDS (Oxford

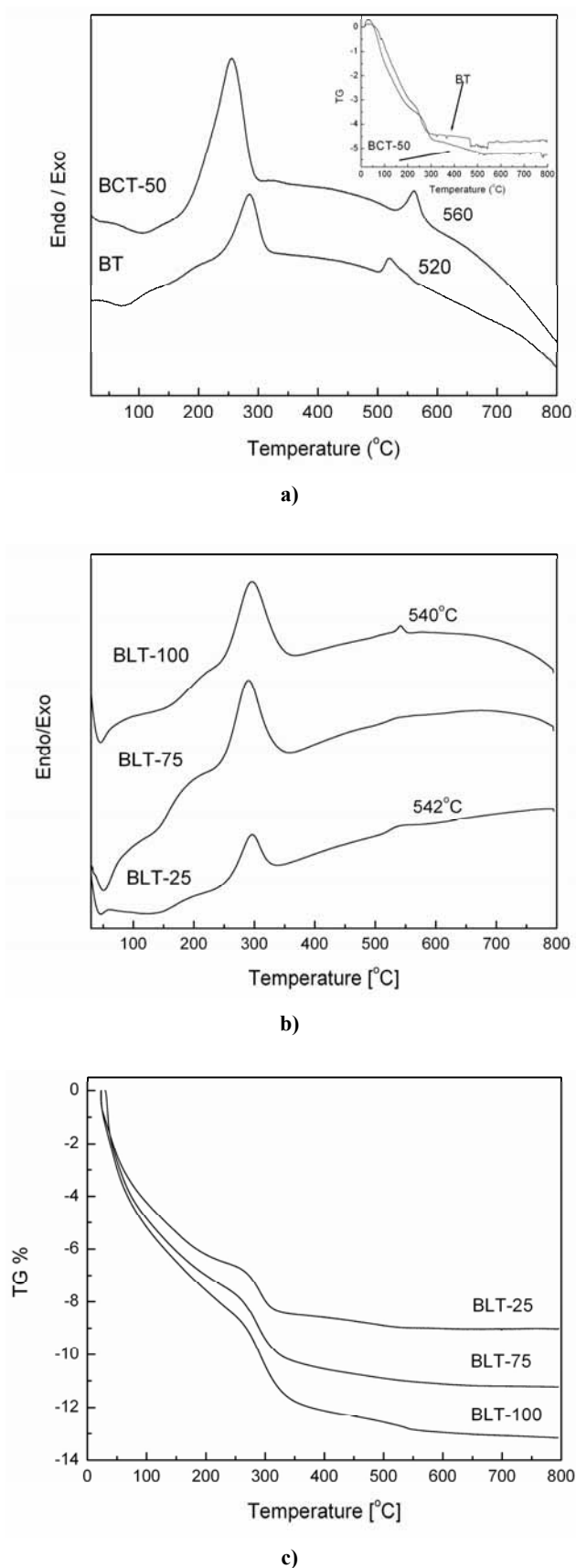
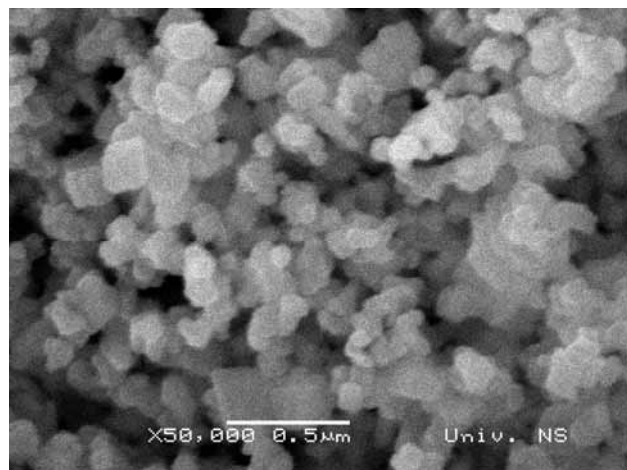
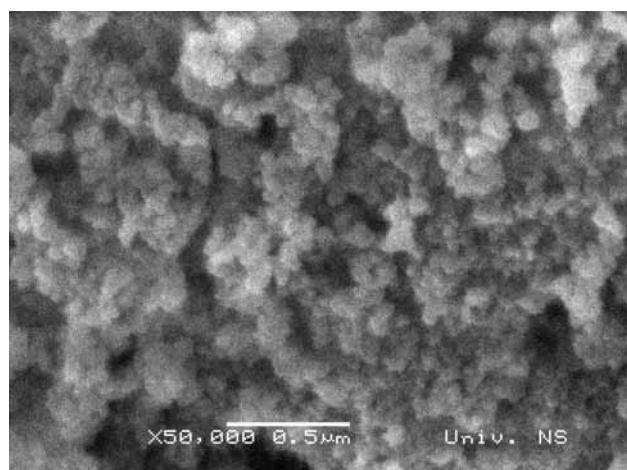


Figure 1. (a) DTA and TG curves of as-synthesized bismuth titanate BT and BCT-50 powders; (b) DTA curves of as-synthesized bismuth titanate BLT powders; (c) TG curves of as-synthesized bismuth titanate BLT powders

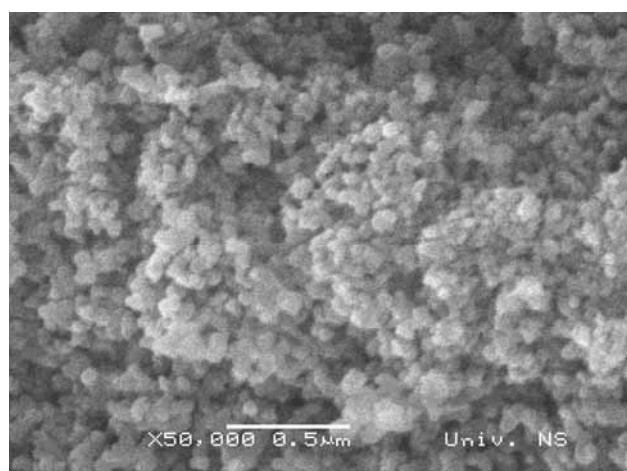
Instruments), respectively. X-ray diffraction (Philips 70, $\text{CuK}\alpha$) for 2θ in the range of 10° to 60° was used to confirm crystalline structure of the calcined powders. The phase structure of the bismuth titanate based ceramics was analyzed by XRD method and the microstructure was observed by SEM. Density of sintered samples was measured by Archimedes method using distilled water.



a)



b)



c)

Figure 2. SEM micrographs of: a) bismuth-titanate, BT, b) Ce- bismuth-titanate, BCT-100 and c) La- bismuth-titanate, BLT-100 nanopowders

III. Results and discussion

Thermal analyses were performed in order to determine the crystallization temperature required to obtain bismuth titanate phase. DTA results of as-synthesized BT, BCT and BLT nanopowders are plotted in Fig. 1. As shown in Fig. 1a and 1b two pronounced exothermic peaks can be observed on the DTA curves for the mentioned powders. The first exothermic peak between 200 and 300°C , which is in correlation with the main weight loss on TG curves (Fig. 1a and 1c), can be attributed to decomposition of residual organics and nitrates. The second exothermic effect, observed around 520°C for the bismuth titanate powder without cation addition (BT), can be attributed to crystallization of bismuth titanate [10]. The DTA and TG data of La and Ce modified powders indicate that this exothermic peak related to the crystallization process is shifted to higher temperatures, i.e. ~ 540 and $\sim 560^\circ\text{C}$, for the BLT and BCT samples, respectively. On the other hand different amounts of La or Ce used for the substitution of Bi ions did not have significant influence on the position of the exothermic peak on the DTA curves. According to the results of thermal behaviour the as-synthesized powders were calcined at 600°C for 1h.

All as-synthesized powders consisted of very fine particles with the size in the nanometer range and with relatively high values of specific surface areas ($\sim 160 \text{ m}^2/\text{g}$). After calcination a rapid drop in the specific surface area in all powders was observed probably attributable to structural changes and particle coarsening. Influence of Ce and La addition on the specific surface area is significant compared to the values of $15.5 \text{ m}^2/\text{g}$ for the pure bismuth titanate. Calcined powders with La had similar values of specific surface area of $\sim 35 \text{ m}^2/\text{g}$ for all ranges of x , while the specific surface area of the Ce doped powders had a tendency to increase with an increase of Ce content. According to micrographs of the calcined powders (Fig. 2), a common characteristic of all three powders is that they are formed by agglomerates of fine equiaxial-shaped particles. As it can be seen from these micrographs, the powders with the Ce and La additions have unambiguously smaller particle size compared to the BT ones, consistent with the recorded values of specific surface areas based on the BET method.

The differences in the FTIR spectra of the powders calcined at 600°C are compared in the Fig. 3. In this figure, the infrared spectrum of the calcined BT nanopowder is compared to that of the as-synthesized BT nanopowder. After calcinations O-H and C-O stretching bands in the ranges $2800\text{--}3700 \text{ cm}^{-1}$ and $1771\text{--}1250 \text{ cm}^{-1}$ disappeared indicating an absence of water and residual organics and nitrates in the calcined powders. The sharp absorption peaks at 814 and 602 cm^{-1} along with a shoulder at 548 cm^{-1} and a peak appearing around 400 cm^{-1} are attributed to Ti-O stretching vi-

brations, which are in accordance with the results for $\text{Bi}_4\text{Ti}_3\text{O}_{12}$ reported in literature [11,12]. In addition, the formation of a titanate structure is confirmed with characteristic bands below 830 cm^{-1} . The significant differences in the FTIR spectra among La modified bismuth titanate powders are not as marked except for the gradual disappearance of the shoulder around 548 cm^{-1} and lower intensity of the band around 830 cm^{-1} . On the other hand, as the content of Ce increases dramatic changes of the shape of the spectra below 1000 cm^{-1} can be noticed. The new absorption band at 927 cm^{-1} appears and the intensities of absorption peaks at 814 , 602 and $\sim 400\text{ cm}^{-1}$ become weaker or disappear. These changes are most probably attributable to significant changes in the structure as a result of Ce addition. These results lead to the conclusion that the addition of La does not have so strong influence on the crystalline structure of bismuth titanate as does the addition of Ce.

X-ray diffraction patterns shown in Fig. 4 reveal more information about the structure and influence of Ce and La addition on the crystallinity of the powders. According to the diffraction data of BT powder the presence of single bismuth titanate phase is detected after calcinations of the as-synthesized powder at 600°C for 1 hour. This result is in agreement with the data obtained by differential thermal analyses and published literature [10,11]. It is interesting to note that XRD peaks at 2θ angles of $\sim 32^\circ$, $\sim 40^\circ$ and $\sim 58^\circ$ are unseparated, indicating that the calcined unmodified powder (sample BT) has tetragonal structure. Since tetragonal $\text{Bi}_4\text{Ti}_3\text{O}_{12}$ is stable only above Curie temperature, the presence of tetragonal structure at room temperature could be due to kinetics [11] and/or size effect [13]. As can be seen in Fig. 4, influences of the addition of La and Ce on the crystalline structure of bismuth titanate are significantly different. While powder with La (BLT-25) has a bismuth-layered structure, XRD data of the three other La modified powders (BLT-50, BLT-75 and BLT-100) in addition to the Aurivillius bismuth titanate layered structured, revealed the presence of cubic pyrochlore phase as the second phase. XRD patterns of these powders showed that the solid solution is free of La-rich phase as well as the shift of the peak position occurred with addition of La. These facts indicate that La enters the bismuth titanate causing the change of the crystal structure. On the other hand, the pyrochlore phase is observed in all samples with a more pronounced impact for the samples with Ce than for those with La. It is worth noting that the XRD pattern of the powder with the highest amount of Ce (sample BCT-100) revealed the existence of a pyrochlore phase without any other detectable bismuth titanate phase. This is very important as it is known that the bismuth titanate pyrochlore phase is a metastable phase existing only in a narrow range of temperature [6]. The presence of a pure pyrochlore phase could be explained by its stabilization due

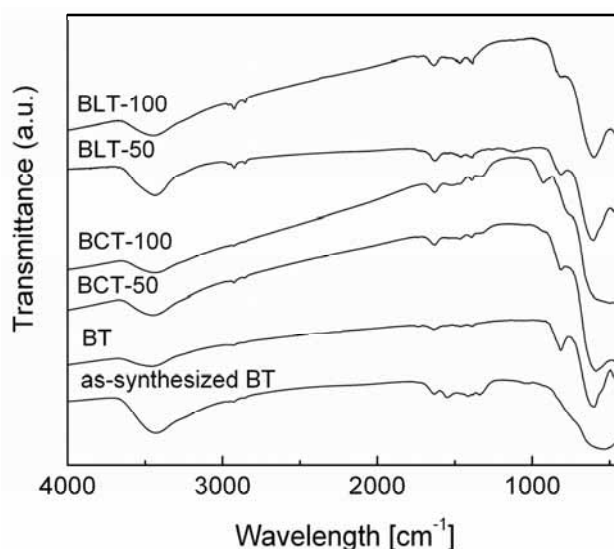


Figure 3. FTIR spectra of powders with different amount of Ce/La ($x=0, 0.5$ and 1) calcined at $600^\circ\text{C}/1\text{h}$

to incorporation of cerium ions in the titanate structure. Details of diffraction patterns of the Ce-modified bismuth titanate powders as well as the role of Ce in the stabilization of the pyrochlore phase were discussed in an earlier paper [14]. Quality analyses of the calcined samples obtained by EDS (Fig. 5) showed the presence of Ce and La in all powders where these ions were added at the beginning of synthesis. This means that Ce and/or La are not washed out during centrifuging, but remains in the structure of the powders.

Recent studies indicate that La^{3+} , as a rare earth cation can substitute Bi^{3+} not only at the 12-fold A site of perovskite block, but partial cation mixing is possible at M and A sites. The size mismatch existing between fluorite-like $[\text{M}_2\text{O}_2]^{2+}$ units and perovskite-like slabs induces strain in the bismuth titanate structure. One way in which this strain can be relieved is octahedral tilting in the room temperature structure of $\text{Bi}_4\text{Ti}_3\text{O}_{12}$ and low-

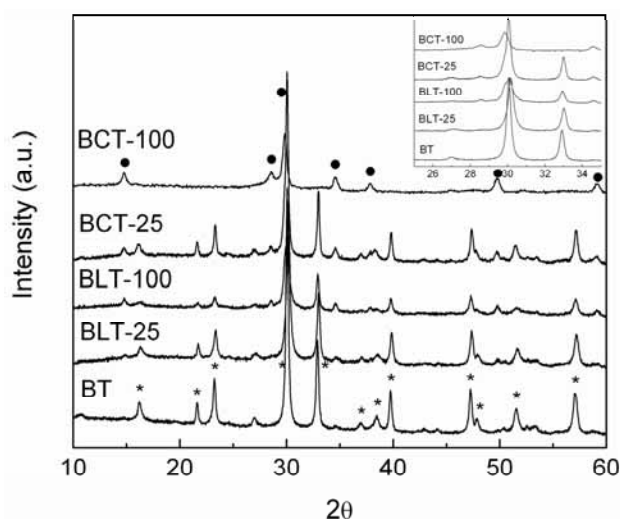


Figure 4. XRD patterns of powders with different amount of Ce and La ($x=0, 0.25$ and 1) calcined at $600^\circ\text{C}/1\text{h}$, bismuth titanate phase (*) and pyrochlore phase (●)

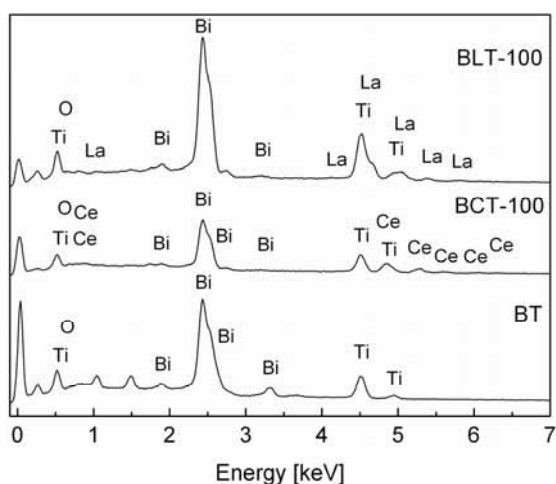


Figure 5. EDS results, quality analyses, of calcined powders: BT, BLT-100 and BCT-100

ering of symmetry from tetragonal to orthorhombic or monoclinic. Besides the octahedral tilting, partial cation mixing at M and A sites, which is referred to as the cation disorder, is suggested as the second type of mechanism for the relief of the inherent strain. Earlier data indicate that for the La content ($x < 1$) octahedral distortion is the most probable mechanism. As the La content increases the degree of M/A cation disorder becomes more pronounced as in the case of $\text{Bi}_3\text{LaTi}_3\text{O}_{12}$ and $\text{Bi}_2\text{La}_2\text{Ti}_3\text{O}_{12}$ reported by Hervoches and Chu [1,2]. On the other hand, the position of Ce in the structure of bismuth titanate is different. Among lanthanide metals Ce can change its oxidation states easily between +3 and +4 and has the characteristic of oxygen storage [15]. It can be expected that Ce ions preferably occupy Bi-site in the bismuth titanate ceramics due to a similar ionic radii and the fact that at higher temperature ($> 730^\circ\text{C}$) Ce^{4+} cation is usually reduced to Ce^{3+} . In this valent state a part of the Ce ions enters the crystal structure at Bi-site, similar to A-site substitution in perovskite oxides. Howev-

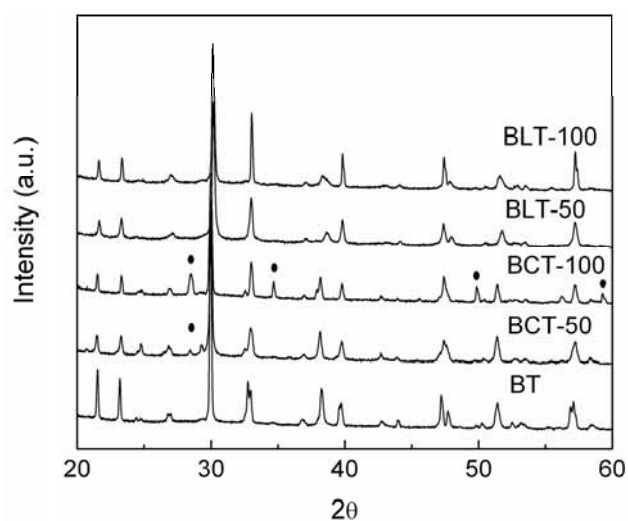


Figure 6. XRD patterns of BT, BCT-50, BCT-100, BLT-50 and BLT-100 sintered at $1050^\circ\text{C}/2\text{h}$ (● - pyrochlore phase)

er, in spite of the large difference in the ionic radii of Ce^{4+} (0.087 nm) and Ti^{4+} (0.0605 nm), in some cases the Ce^{4+} ion can partially substitute the Ti^{4+} ion located at the center of the oxygen octahedron of perovskite type unit [4,16]. Thus, we assume that when Ce is added into a bismuth titanate structure, it will most probably replace Bi^{3+} ions, but it could be introduced also into B-sites, i.e. on the Ti^{4+} position, depending on oxygen states of Ce ion. This increases off-center displacement because the radius of Bi^{3+} (0.093 nm) is smaller than that of Ce^{3+} (0.101 nm) and the radius of Ti^{4+} is much smaller even than that of Ce^{4+} (0.087 nm).

X-ray diffraction patterns of samples $\text{Bi}_4\text{Ti}_3\text{O}_{12}$, $\text{Bi}_{4-x}\text{Ce}_x\text{Ti}_3\text{O}_{12}$ and $\text{Bi}_{4-x}\text{La}_x\text{Ti}_3\text{O}_{12}$ sintered at 1050°C for two hours with different values of x are illustrated in Fig. 6. XRD data for the ceramic sample BT revealed the existence of single bismuth titanate phase. However, for Ce-modified bismuth titanate ceramics, there are small amounts of pyrochlore phase for all values of x . On the other hand patterns of ceramics with La addition showed the presence of only a bismuth layer-structured phase.

The microstructure of the bismuth titanate-based ceramics sintered at 1050°C is shown in Fig. 7. All of these materials consist of plate-like grains as observed in the micrographs of the fracture surface of the samples BT, BCT-50 and BLT-50. Density of the pure bismuth titanate ceramics was around 93% of theoretical density, while the Ce and La modified ceramics revealed very dense material, above 95% of theoretical density. On increasing the content of La in the obtained ceramics, there is a tendency for the grains to become smaller with pronounced plate-like morphology. In contrast, the major feature apparent from the micrographs of the samples with Ce is the fracture occurring through the large number of grains. The existence of transgranular fracture in the samples with Ce is probably attributable to distribution of Ce in the boundary region.

IV. Conclusions

Very fine and agglomerated $\text{Bi}_{4-x}\text{Ce}_x\text{Ti}_3\text{O}_{12}$ and $\text{Bi}_{4-x}\text{La}_x\text{Ti}_3\text{O}_{12}$ ($x \leq 1$) nanopowders were prepared using modified sol-gel method. Powders calcined at 600°C had different phase composition, depending on the substituting ion and quantity of the same. In addition to Aurivillius layered structure, a small amount of cubic pyrochlore phase was detected in the La modified powders, while this second phase was much more pronounced in the powder with Ce addition. The pure pyrochlore structure was detected in the powder with the highest amount of Ce (BCT-100) what leads to the conclusion that addition of Ce stabilizes the formation of this phase. This different influence of cerium and lanthanum could be explained by the incorporation of their ions on the different sites in the titanate structure. Bismuth titanate based ceramics, sintered at $1050^\circ\text{C}/2\text{h}$, had densities above 93% of theoretical density and characteris-

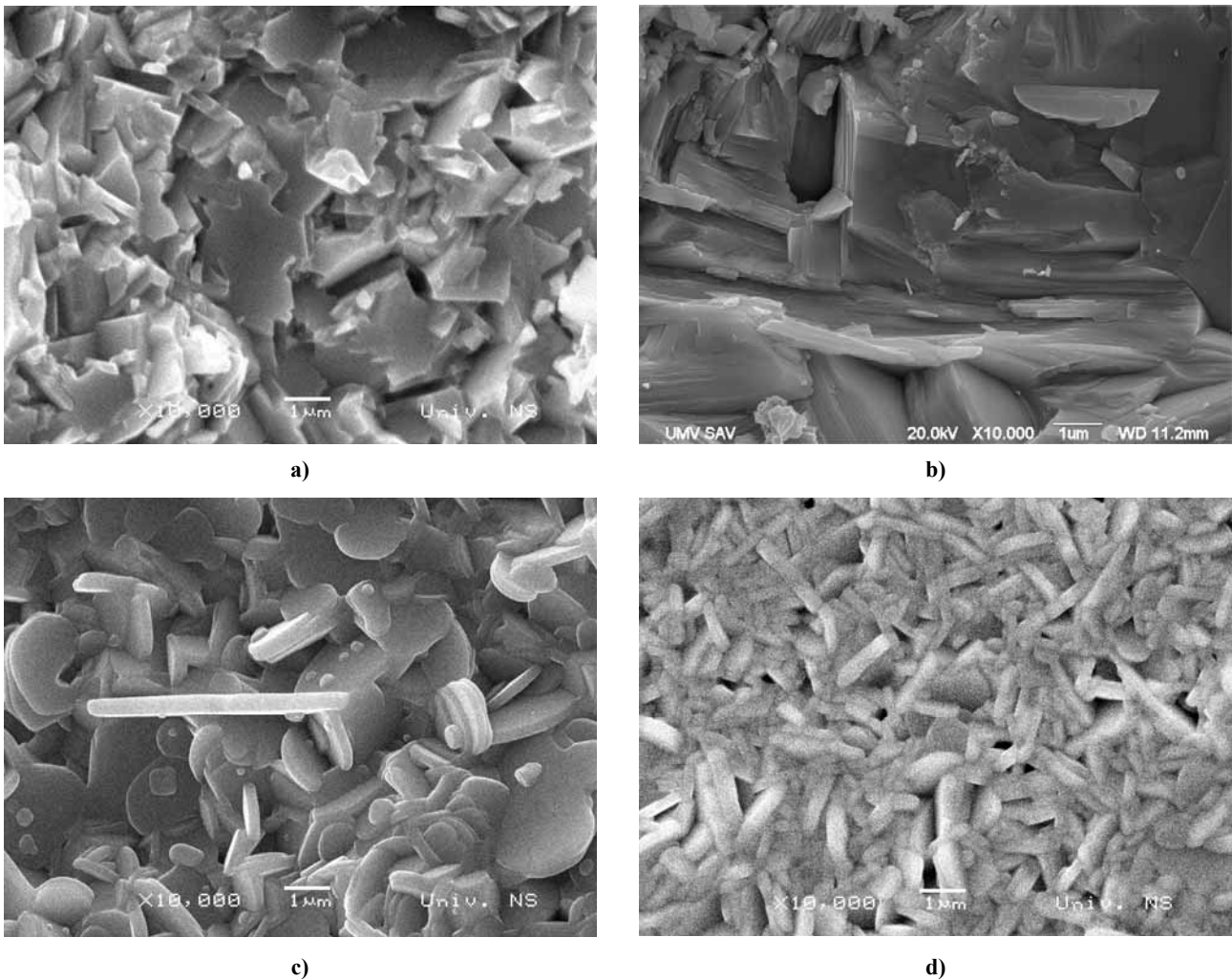


Figure 7. SEM micrographs of the fracture surfaces of the samples sintered at 1050°C for 2h: a) BT, b) BCT-50, c) BLT-50 and d) BLT-75

tic plate-like grain morphology. Small quantity of cubic pyrochlore phase was detected only in the Ce modified bismuth titanate ceramics. On the other hand, lanthanum addition caused formation of smaller grain size with pronounced plate-like morphology.

References

1. C.H. Hervoches, P. Lightfoot, "Cation disorder in three-layer Aurivillius phases: structural studies of $\text{Bi}_{2-x}\text{Sr}_{2+x}\text{Ti}_{1-x}\text{Nb}_{2+x}\text{O}_{12}$ ($0 < x < 0.8$) and $\text{Bi}_{4-x}\text{La}_x\text{Ti}_3\text{O}_{12}$ ($x=1$ and 2)", *J. Solid State Chem.*, **153** (2000) 66–73
2. M.W. Chu, M.T. Caldes, L. Brohan, M. Ganne, A. M. Marie, O. Joubert, Y. Piffard, "Bulk and surface structures of the Aurivillius phases: $\text{Bi}_{4-x}\text{La}_x\text{Ti}_3\text{O}_{12}$ ($0 \leq x \leq 2.00$)", *Chem. Mater.*, **16** (2004) 31–42.
3. M. Villegas, T. Jardiel, A.C. Caballero, J.F. Fernandez, "Electrical properties of bismuth titanate based ceramics with secondary phase", *J. Electroceram.*, **13** (2004) 543–548.
4. S.K. Singh, H. Ishiwara, "Site engineering in chemical-solution-deposited $\text{Bi}_{3.25}\text{La}_{0.75}\text{Ti}_3\text{O}_{12}$ thin films using Ce, Zr, Mn and Si atoms", *J. Sol-Gel Sci. Techn.*, **42** (2007) 231–238.
5. A.Z. Simoes, C. Quinelato, A. Ries, B.D. Stojanovic, E. Longo, J.A. Varela, "Preparation of lanthanum doped $\text{Bi}_4\text{Ti}_3\text{O}_{12}$ ceramics by the polymeric precursor method", *Mater. Chem. Phys.*, **98** (2006) 481–485.
6. A. Hector, S.B. Wiggin, "Synthesis and structural study of stoichiometric $\text{Bi}_2\text{Ti}_2\text{O}_7$ pyrochlore", *Solid State Chem.*, **177** (2004) 139–145.
7. J.S. Patwardhan, M.N. Rahaman, "Compositional effects on densification and microstructural evolution of bismuth titanate", *J. Mater. Sci.*, **39** (2004) 133–139.
8. V. Ravi, S. Adyanthaya, M. Aslam, S. Pethkar, V.D. Choube, "Synthesis of bismuth tin pyrochlore", *Mater. Lett.*, **40** (1999) 11–13.
9. L.A.J. Garvie, H. Xu, Y. Wang, R.L. Putnam, "Synthesis of $(\text{Ca}, \text{Ce}^{3+}, \text{Ce}^{4+})_2\text{Ti}_2\text{O}_7$: a pyrochlore with mixed-valence cerium", *J. Phys. Chem. Solids*, **66** (2005) 902–905.
10. S.H. Ng, J. Xue, J. Wang, "Bismuth titanate from mechanical activation of chemically coprecipitated precursor", *J. Am. Ceram. Soc.*, **85** (2002) 2660–2665.

11. Y. Kan, P. Wang, Y. Li, Y. Cheng, D. Yan, “Low-temperature sintering of $\text{Bi}_4\text{Ti}_3\text{O}_{12}$ derived from co-precipitation method”, *Mater. Lett.*, **56** (2002) 910–914.
12. D. Chen, X. Jiao, “Hydrothermal synthesis and characterization of $\text{Bi}_4\text{Ti}_3\text{O}_{12}$ powders from different precursors”, *Mater. Res. Bull.*, **36** (2001) 355–363.
13. W.S. Cho, E. Hamada, “Synthesis of ultrafine BaTiO_3 particles from polymeric precursor: their structure and surface property”, *J. Alloys Compd.*, **266** (1998) 118–122.
14. N. Pavlovic, V.V. Srdic, “Synthesis and structural characterization of Ce doped bismuth titanate”, *Mater. Res. Bull.*, **44** (2009) 860–864.
15. M.K. Jeon, H.J. Chung, K.W. Kim, K.S. Oh, S.I. Woo, “Ferroelectric properties of $\text{Bi}_{3.25}\text{Ce}_{0.75}\text{Ti}_3\text{O}_{12}$ thin films prepared by a liquid source misted chemical deposition”, *Thin Solid Films*, **489** (2005) 1–4.
16. D.-Y. Lu, M. Toda, “High-permittivity double rare-earth-doped barium titanate ceramics with diffuse phase transition”, *J. Am. Ceram. Soc.*, **89** (2006) 3112–3123.